

Article

Pulse Detonation Assessment for Alternative Fuels

Muhammad Hanafi Azami * and Mark Savill

Propulsion Engineering Centre, School of Aerospace Transport & Manufacturing, Cranfield University, Cranfield MK43 0AL, UK; mark.savill@cranfield.ac.uk

* Correspondence: m.azami@cranfield.ac.uk

Academic Editors: Antonio Ficarella and Maria Grazia De Giorgi

Received: 28 November 2016; Accepted: 9 March 2017; Published: 15 March 2017

Abstract: The higher thermodynamic efficiency inherent in a detonation combustion based engine has already led to considerable interest in the development of wave rotor, pulse detonation, and rotating detonation engine configurations as alternative technologies offering improved performance for the next generation of aerospace propulsion systems, but it is now important to consider their emissions also. To assess both performance and emissions, this paper focuses on the feasibility of using alternative fuels in detonation combustion. Thus, the standard aviation fuels Jet-A, Acetylene, Jatropa Bio-synthetic Paraffinic Kerosene, Camelina Bio-synthetic Paraffinic Kerosene, Algal Biofuel, and Microalgae Biofuel are all assessed under detonation combustion conditions. An analytical model accounting for the Rankine-Hugoniot Equation, Rayleigh Line Equation, and Zel'dovich–von Neumann–Doering model, and taking into account single step chemistry and thermophysical properties for a stoichiometric mixture, is applied to a simple detonation tube test case configuration. The computed pressure rise and detonation velocity are shown to be in good agreement with published literature. Additional computations examine the effects of initial pressure, temperature, and mass flux on the physical properties of the flow. The results indicate that alternative fuels require higher initial mass flux and temperature to detonate. The benefits of alternative fuels appear significant.

Keywords: pulse detonation engine; alternative fuels; biofuels; pressure-gain combustor; propulsion

1. Introduction

In the very early development of jet-propulsion engines, it was known from the thermodynamic analysis cycle that an engine based on a constant-volume combustion process achieves higher thermodynamic efficiency than a constant pressure engine. The earliest non-piston-engine-type prime mover employing constant volume combustion with a deflagrative and not a detonative reaction was the Holzwarth gas turbine manufactured by Brown-Boveri (now ABB) in Switzerland during the early part of the last century, but its success was limited [1]. Eidelman, Grossmann, and Lottati [2] and Ma, Choi, and Yang [3] have summarized that the first reported work on intermittent detonation is attributed to Hoffman in 1940, using acetylene and benzene as fuels with oxygen. After the work was terminated during World War II, Nicholls and co-workers reinitiated the effort in the 1950s by experimenting with a series of single- and multiple-cycle detonation experiments with different mixtures of hydrogen, oxygen, acetylene, and air in a six-foot tube. The Naval Postgraduate School (NPS) reexamined the pulse detonation engines (PDE) concept in the late 1980s and successfully demonstrated the self-aspirating feature of air breathing PDE using ethylene/oxygen and ethylene/air mixtures. Since then, there has been a growing interest in PDEs as a propulsion technology for both air breathing and rocket systems.

In the context of repetitive mode detonative burning to develop thrust [4–6], PDEs represent one of the pressure-rise unsteady propulsion systems, which differ from conventional propulsion

frameworks [3,7]. This potential alternative combustor technology introduces a rapid detonation wave as a more thermodynamically efficient means for converting chemical to mechanical energy and thus generating far higher kinetic energy [8–11] compared to the normal deflagration combustion process [12]. PDE offers numerous potential advantages; however, it also suffers from several drawbacks too. A list of advantages and disadvantages are summarized in Table 1. The theory, operational considerations, and research done for PDE will be described in the next section.

Table 1. PDE Advantages and Disadvantages.

Advantages	References
High energy heat release rate and propulsive thrust.	[13–15]
High specific impulse compared with ramjet under similar operating conditions.	[13]
Simple in manufacture and operation, less moving parts, low cost, high range flight Mach numbers, weight reduction, and more compact.	[14,16–22]
High thermodynamic cycle efficiency, operation stability, and reliability.	[3,11,14,19,20]
Improved fuel efficiencies in high speed and longer ranges.	[4,14,23]
Can be used in conjunction with other developing technologies (flexible).	[4,14,22]
Disadvantages	
Noisy.	[14]
Liquid fuelled PDEs are bulkier.	[24]
Possessed a noticeable total pressure loss during both the filling (valve) and detonation portion of the cycle.	[4,25]
Introduced an additional loss mechanism with obstacles, which required cooling for increased longevity.	[25]
Thrust density, or thrust-per-unit cross-sectional area, is lower than that of a turbo-ramjet engine.	[4]
Very low thrust and Specific Fuel Consumption (SFC) at low speeds.	[4]
Requires a long runway for takeoff.	[4]
Needs to carry an additional mixture or have an on board oxygen generator.	[26]

Awareness of environmental and energy crises has prompted tremendous efforts such as the Clean Sky JTI Projects by the European countries, The Environmentally Responsible Aviation Project (ERA) by National Aeronautics and Space Administration (NASA), and several more. The aviation industries have shifted their strategy to use alternative fuels based on biofuels. The use of drop-in fuels and blended fuels in aircraft engines has significantly attracted the attention and interest of engineers and researchers throughout the world. Drop-in fuels need minor or no modifications at all in the aircraft engine in service. It offers a future ‘greener’ aircraft and less dependency on crude oil. Following the successful flights of many commercial aircraft running with different biofuels, these have become a viable choice to sustain the environment as well as conserve energy. However, there are shortcomings associated with the use of biofuels alone in aircraft engines, such as in terms of thermodynamic efficiency and performance. Running an engine using biofuels with pressure-rise combustors would certainly be a good choice and strategy to satisfy greener technology with better performance. Indeed, it is believed that such alternative combustor technologies fueled by alternative fuels could meet the 2050 emissions targets plan for aviation.

Four biofuels, namely Jatropha Bio-synthetic Paraffinic Kerosene (JSPK), Camelina Bio-synthetic Paraffinic Kerosene (CSPK), Microalgae Biofuel, and Algal Biofuel have been evaluated as pure fuels and are compared here with conventionally used kerosene and acetylene fuels. These particular biofuels were chosen because of previously reported successful use in conventional engine test flight programs and because their fuel properties are available in the published literature, as listed in the

Appendix A. The 3rd and 4th Generation' biofuels derived from "algae-to-biofuels" and microalgae biofuel technologies are based on algae biomass processing for biofuel production and metabolic engineering from oxygenic photosynthetic microorganisms [27]. These are considered to provide a technically viable alternative energy resource, overcoming the major drawbacks associated with first and second generation biofuels [28]. The other main feature of such algae and microalgae-based biofuels is they have the highest oil yield compared to other types of feedstocks because of their unique fast growing capabilities. Microalgae, in particular, have been suggested as potential candidates for fuel production, capable of meeting the global and sustainable demand for transport fuels [29] because of a number of key advantages, including higher energy yields per hectare, higher photosynthetic efficiency, higher biomass production, higher growth rates, and a non-requirement of agricultural land compared to other energy crops [30,31]. (Some microalgae have also been reported as good producers of hydrogen which offers higher energy potential and almost no pollution [32]). Microalgae biofuel has properties similar to those of petro-diesel in terms of density, viscosity, flash point, cold flow, and heating value. None of the other potential sources of biodiesel present as realistic an option for replacing petro diesel sustainably as microalgae do [33].

However, to date, almost no efforts have been made to study the use of such alternative fuels under detonation combustion conditions. Although studies have been made of heavy-hydrocarbon fuel such as Jet Propellant (JP10), none have been made of other commercialized alternative fuels. Since alternative fuels are targeted to be used in the near future, it is certainly worth exploring the wider capability of these fuels as well. The uniqueness of this paper is to assess the behavior of such alternative fuels in terms of physical and chemical properties for changes in the different initial conditions. This study only uses one-step chemistry reactions for a start in order to make a straight comparison between different fuels and to assess whether these might be sufficiently accurate to be useful. Thus, remaining differences within the experiment are most probably due to not using full multi-step chemistry and leave open this extension for further investigations and improvements.

2. Theory, Process and Previous Works on PDE

PDE detonation is modeled as a normal shock wave or Zel'dovich–von Neumann–Doering (ZND) detonation wave, advancing into the undisturbed fuel-air mixture of a uniform cross-sectional area tube, which is almost at rest for combustor entry conditions [34]. This is then followed by Rayleigh type combustion [35]. The whole process satisfies the Chapman-Jouguet (CJ) condition, which requires that the local Mach number at the termination of the heat expansion region be choked [34]. CJ theory requires chemical reactions to be represented by heat discharge in an infinitesimally thin shock front that brings the material from a starting state on the inert Hugoniot line to a subsequent CJ point state [20]. The CJ point also forms a tangent from the initial to final state on a Pressure-Volume diagram (p - v diagram) equivalent to the Rayleigh heating process. It is difficult to evaluate the relative performance of air-breathing PDEs with respect to conventional steady-flow propulsion systems without performing a full unsteady computational analysis because of the intrinsically unsteady nature of the flow field due to the detonation process [16,36,37].

In a conventional Brayton cycle, the heat injection process has the maximum exergy, which is fixed by the compressor's delivered pressure and the maximum temperature allowed by the cycle. Therefore, the exergy can be increased if the heat injection process follows a different thermodynamic cycle path [38]. The thermodynamic cycle of ideal PDE is similar to the ideal Brayton cycle, while the Humphrey cycle is considered a modification to the Brayton cycle in which the constant-pressure heat addition process is replaced by a constant-volume heat addition process [34]. The Humphrey cycle is much more efficient than the Brayton cycle, in which a very rapid burning takes place. Due to the rapidity of the process, there is not enough time for pressure equilibration, and the overall process is thermodynamically closer to a constant volume process than to the constant pressure process typical of conventional propulsion systems [39]. The thermodynamic efficiency of Chapman–Jouget detonation has minimum entropy generation along the Hugoniot curve as compared to other combustion modes,

which appear to have a potential thermodynamic advantage [13,40]. In general, the Humphrey cycle consists of four processes. The first is an isentropic compression. This compression occurs ahead of the detonation wave in PDEs. Compression is followed by constant volume combustion. Another isentropic process expands the combustion products back to atmospheric pressure. In the PDE, the rarefaction waves cause this expansion process. Finally, an isobaric process brings the cycle back the start of the cycle. Figure 1 illustrates the detonation process in order.

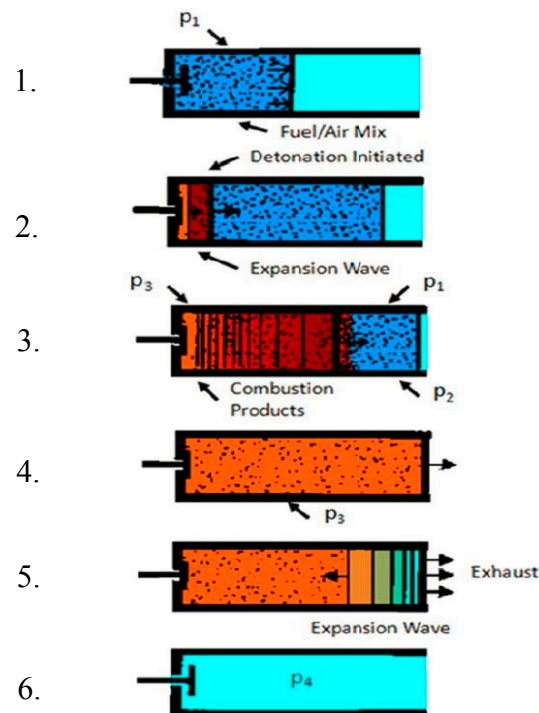


Figure 1. Detonation process adapted from Blanco [38], with permission from Cranfield University, 2014.

Researchers throughout the world have clearly already done quite extensive work on PDE. In addition Ma, Choi, and Yang [41] have summarized the findings of both numerical and experimental work on air breathing PDE using hydrogen fuel in a review article. Figure 2 attempts to summarise by key words all the topics covered across their identified themes and illustrates the wide breadth of PDE research. Roy et al. [42] and Kailasanath [39,43,44] have also presented detailed review discussions of PDE work, so we will not repeat these here. The present work can be categorized as a first examination of the applicability and feasibility of the selected alternative fuels for detonation combustion. It should be noted, however, that two previous numerical studies have been conducted investigating the detonation characteristics of biofuel and the feasibility of biogas; by Shimada et al. [45], using bio-ethanol, and Dairobi et al. [46], using biogas. Shimada et al. utilized STANJAN for 2D bio-ethanol chemical reactions to study the two-phase detonation of bio-ethanol/air, which showed that the biofuel resulted in a smaller cell size. Meanwhile, the biogas studies suggested that this requires supplementary additives for higher detonation pressure. Our own numerical work utilises ZND Theory and CJ Theory in a zero dimensional analysis under a few basic assumptions, which will be discussed in the theoretical model framework. As a first attempt, the approach was to employ single tube, single phase, and single cycle processes. The theoretical formulation and numerical framework will be discussed in the following section.

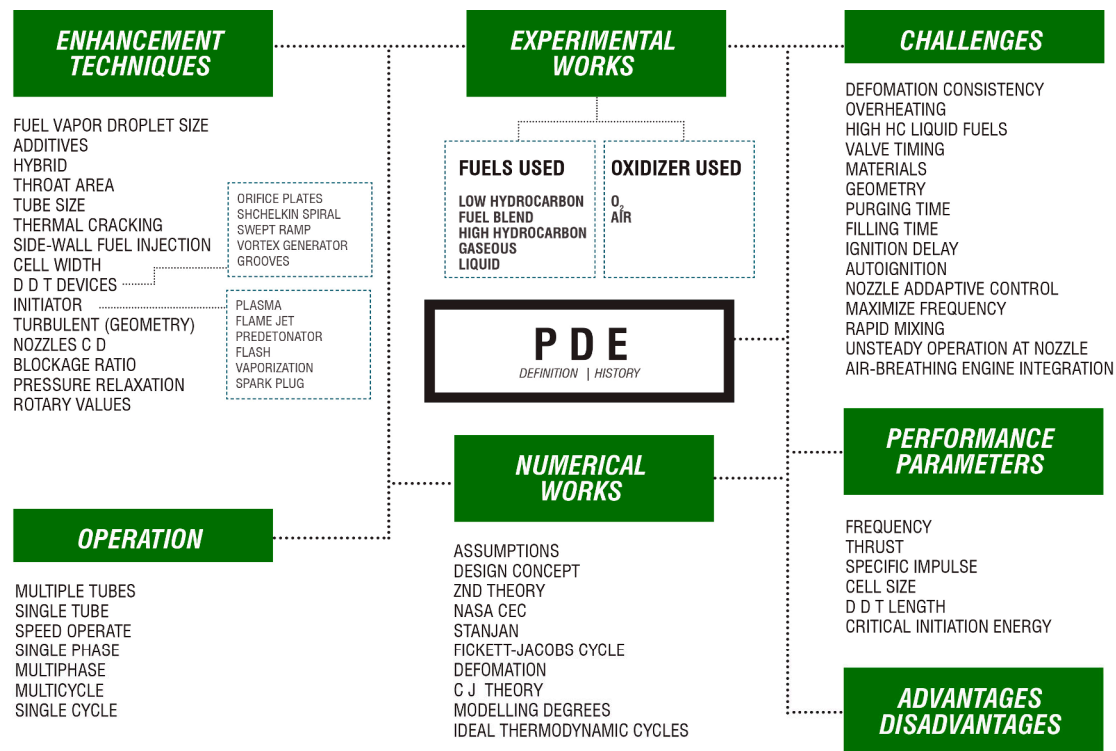


Figure 2. Overview of pulse detonation engines (PDE).

3. Methodology: Theoretical Formulation and Numerical Framework

The model adopted here uses an open-ended constant-area tube geometry in a single cycle operation. It incorporates appropriate expressions, including the Rankine-Hugoniot Equation, Rayleigh Line Equation, species mole and mass fraction of the reactants, enthalpies-of-formation, and ideal-gas normal shock equations. The computational results from our analyses have been verified using the available limited published data from the literature to ensure the consistency of our model across an acceptable range of cases. Five key simplifying assumptions have been made in our work: upstream and downstream boundaries are included in the control volume, with no temperature or species concentration gradients; there is uniform one-dimensional flow under adiabatic conditions; body forces, dissociation of products, and atomization of fuel are neglected; and only the normal shock relation is considered. In addition, although there are many variations in the molecular structures of these alternative fuels, consideration of such variability in the characteristics of the fuels is also neglected, and the analysis is based solely on the information given in the Appendix A. Figure 3 illustrates the different stages for the calculations below.

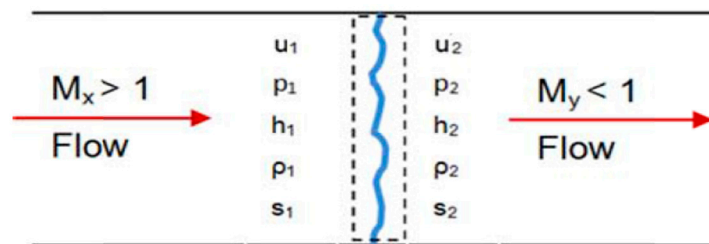


Figure 3. Illustrations of different stages adapted from Blanco [38], with permission from Cranfield University, 2014.

One-dimensional analysis with the variation of mass flux, initial temperature, and pressure is calculated from the conservation of mass and momentum. Thus the Rayleigh line yields the following relationship:

$$\frac{P_2 - P_1}{\frac{1}{\rho_2} - \frac{1}{\rho_1}} = \frac{P_2 - P_1}{v_2 - v_1} = -\dot{m}''^2 \quad (1)$$

Combining conservation of mass, momentum, and energy with heat addition yields:

$$\frac{\gamma}{\gamma - 1}(P_2 v_2 - P_1 v_1) - \frac{1}{2}(P_2 - P_1)(v_1 + v_2) - q = 0 \quad (2)$$

From the Rayleigh Line, P_2 is:

$$P_2 = P_1 + \dot{m}''^2(v_1 - v_2) \quad (3)$$

Substituting into the Rankine-Hugonit Curve yields:

$$\frac{\gamma}{\gamma - 1}[(P_1 + \dot{m}''^2(v_1 - v_2))v_2 - P_1 v_1] - \frac{1}{2}((P_1 + \dot{m}''^2(v_1 - v_2)) - P_1)(v_1 + v_2) - q = 0 \quad (4)$$

Expanding and converting to the quadratic equation:

$$av_2^2 + bv_2 + c = 0 \quad (5)$$

where

$$a = \frac{1 + \gamma}{2(1 - \gamma)} \dot{m}''^2 \quad (6)$$

$$b = \frac{\gamma}{\gamma - 1} (P_1 v_1 + \dot{m}''^2 v_1) \quad (7)$$

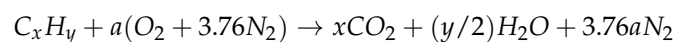
$$c = \frac{\gamma}{1 - \gamma} P_1 v_1 - 1/2 \dot{m}''^2 v_1^2 - q \quad (8)$$

$$v_1 = \frac{R_1 T_1}{P_1} \quad (9)$$

And solving for v_2 :

$$v_2 = \frac{-b \pm \sqrt{b^2 - 4ac}}{2a} \quad (10)$$

P_2 , $V_{x,2}$, T_2 , c_2 , and M_2 for every v_2 are calculated accordingly. Next, detonation velocity in stoichiometric conditions and the gas-mixture properties at the shock front (state 2') are estimated by applying a stoichiometric relation.



Every species mole and mass fraction are calculated, and thermochemical properties such as specific heat, gas constant, and specific heat ratio are obtained using these relations:

$$c_{p,1} = \frac{\sum_{state\ 1} \chi_i \bar{c}_{p,i}}{MW_1} \text{ and } c_{p,2} = \frac{\sum_{state\ 2} \chi_i \bar{c}_{p,i}}{MW_2} \quad (11)$$

$$R_2 = \frac{R_u}{MW_2} \text{ and } \gamma_2 = \frac{c_{p,2}}{c_{p,2} - R_2} \quad (12)$$

Heat formation, q , is calculated using enthalpies-of-formation in the tabulated table, which is converted to a mass basis.

$$q \equiv \sum_{state\ 1} Y_i h_{f,i}^0 - \sum_{state\ 2} Y_i h_{f,i}^0 \quad (13)$$

Detonation velocity and temperature at State 2 are determined using:

$$v_D = \left[2\gamma_2 R_2 (\gamma_2 + 1) \left(\frac{c_{p,1}}{c_{p,2}} T_1 + \frac{q}{c_{p,2}} \right) \right]^{1/2} \quad (14)$$

$$T_2 = \frac{2\gamma_2^2}{\gamma_2 + 1} \left(\frac{c_{p,1}}{c_{p,2}} T_1 + \frac{q}{c_{p,2}} \right) \quad (15)$$

Using ideal-gas normal-shock and knowing the mixture specific-heat ratio and Mach number at the initial state, these relations are used to find State 2':

$$\frac{P_{2'}}{P_1} = \frac{1}{\gamma + 1} \left[2\gamma M_1^2 - (\gamma - 1) \right] \quad (16)$$

$$\frac{T_{2'}}{T_1} = \left[2 + M_1^2 (\gamma - 1) \right] \frac{2\gamma M_1^2 - (\gamma - 1)}{(\gamma + 1)^2 M_1^2} \quad (17)$$

$$\frac{\rho_{2'}}{\rho_1} = \frac{(\gamma + 1) M_1^2}{(\gamma - 1) M_1^2 + 2} \quad (18)$$

$V_{x,2'}$ is calculated using the conservation of mass. The State 2 Mach number should be equal to one (upper CJ point).

4. Results and Discussion

4.1. Validation of the Model

Prior to further analysis, the above model has been validated, first against a case study of Turns [47] for acetylene fuel. The same procedures have then been used to evaluate other fuels by respecting the chemical relations established by the molecular formula of these fuels under stoichiometric combustion conditions. Experimental data for liquid hydrocarbon detonation suitable for comparison with our results are quite scarce. Only limited data exist with which just a few comparisons can be made, and no data are available for alternative bio-fuels. Most experiments have been carried out using either hydrogen-oxygen or hydrogen-air reactions because of the ease with which detonation can be initiated. Nevertheless, a parametric validation was attempted in terms of the detonation velocity and pressure gain in the burned state. Only the results for acetylene and kerosene fuels could be validated in this way. Model results for acetylene fuel were compared with the experimental data of Turns [47] and an analytical study by Wintenberger [48], while comparisons for kerosene fuel were made with the analytical study of Wintenberger [48] and the time-dependent Computational Fluid Dynamics (CFD) of Yungster [49], as well as experimental work conducted by Cheatham [50] for a range of fuel droplet sizes. The detonation velocity is taken at the von Neumann spike, while pressure rise is taken as time-averaged. The literature findings were found to be generally comparable to the results obtained from our model calculations for both the detonation velocity and the pressure gained, especially for the acetylene experiments and kerosene computations, as shown in Table 2.

Detonation is also certainly sensitive to variations in the initial conditions (temperature, pressure, mass flux), which are not always sufficiently completely specified for complete comparison. Our initial sensitivity studies suggested that changes in the initial conditions resulted at most in ~10% uncertainty in the predicted detonation velocity. Any dissociation effects are likely to have the other largest effect on the detonation velocity. The detonation velocity is computed from Equation (14), which is based on the numerical approximation that the pressure of the burned state is much greater than the pressure of the unburned state. Detonation ratios of pressure calculated in a burned state over pressure in an unburned state are in the recommended range, see Reference [47], so this approximation is reasonable for the detonation case. However, when dissociation occurs, minor species will be formed, and the species mole and mass fractions of the products will be different, with resulting

different values of heat addition, q , and total specific heat of the burned state (Equations (11) and (13)). From Equation (14), the detonation velocity is a square root function of these dependent variables, and, in the case of dissociation, the total specific heat of the burned state will increase while the heat addition (heat difference of reactant to product) would be less, resulting in lower detonation velocity as suggested by some published experiments and analytical results. In the worst case, a 35% discrepancy can be found between the detonation speed predicted for Kerosene and the published analytical and experimental findings. However, we would point out that the analytical results are based on a simplified method, while the experimental results are also subject to error bars due to measurement and other uncertainties, and the predicted detonation speed is supported by published higher fidelity CFD results [49]. For acetylene, also, our predicted detonation velocity matches exactly a separate published experimental measurement [47] and agrees within 6% with the same analytical analysis [48], such that our model predictions fall within the bounds of these few other available published findings. We believe this suggests that our adopted methodology is an appropriate one, at least for such an initial investigation of biofuel alternatives, which are all predicted to have a very closely similar (3% variation) higher detonation velocity. Clearly other factors, including dissociation of the products, will need to be addressed to fully confirm our findings, but the trends observed seem clear.

Table 2. Validation of the model with analytical and experimental studies.

ACN	Wintenberger [48]	Turns [47]	Model	
V_D (m/s)	1879	1998	1997.95	
P_2 (atm)	19.20	20.6	25.97	
Jet-A	Wintenberger [48]	Cheatham [50]	Yungster [49]	Model
V_D (m/s)	1784	1786	2300	2398.9
P_2 (atm)	18.40	10–33	16–44	28.98

4.2. Conditions for Detonation

Based on the model derived from Section 3, three parameters have been analysed and compared in terms of the pressure ratios, density ratios, and temperature ratios with respect to the underlying initial conditions at different phases in the detonation tube. However, a few essential steps need to be taken to initiate the analysis: first all the fuels considered must achieve detonation velocity, either by raising the mass flux or the initial temperature, and Table 3 shows the minimum initial temperature and mass flux before every alternative fuel can be detonated. These minimum conditions were established as satisfying Equation (10) for which the variables of a , b , and c are functions of pressure, mass flux, specific volume, temperature, heat addition, and specific heat. (It has to be noted that the heavy hydrocarbon fuels, Jet-A, and the biofuels are hard to detonate and need to be pre-heated or accelerated to a high velocity. Microalgae fuel (MA), which requires the highest temperature and mass flux, is seen to be the most difficult to detonate and Acetylene (ACN) the least. Secondly the flow must be choked at Stage 2, and, thirdly, stoichiometric combustion has to be assured.

The thermodynamic parameters are used to faithfully predict the detonation speed and other properties within the range of minimum temperature and mass flux. Generally, for a given reactant pressure and temperature, the thermochemical products and detonation velocity could be estimated from NASA Chemical Equilibrium with Applications (CEA) analysis. However, our analysis uses a different analytical approach by allowing for mole, mass fraction, and enthalpy-of-formation of the reactants using simple chemical relations in combustion. To estimate the detonation velocity requires the estimation of heat addition, q , burned properties, and unreacted mixture specific heat. To obtain these, the compositions of the unreacted and reacted mixtures are first determined. Since the chemical relations of these fuels in stoichiometric combustion are well balanced, the species mole and mass fractions can be determined, and the thermochemical properties during reaction are tabulated in Table 4. These properties are calculated based on the summation of each species, formed to find its

detonation velocity at arbitrary 2' state using a ZND model. It is shown that all biofuels exhibit high heat addition, which is believed to be due to the complex molecular structure of biofuels. Heavy hydrocarbon requires much higher heat addition to break the bonds in the molecule for combustion. Further analysis shows that higher flame temperatures are obtained for these fuels.

Table 3. Minimum initial temperature and mass flux for detonation.

Properties	CAN C_2H_2	JET-A $C_{12}H_{24}$	MA $C_{12}H_{20}O_5N_2$	JSPK $C_{12}H_{26}$	CSPK $C_{12}H_{25.4}$	AL $C_{12}H_{19}O_3N$
T_1 (K)	300	1467	2000	1700	1700	2000
G (kg/s·m ²)	2612	3000	5800	4400	4400	4800
γ_1	1.379	1.267	1.209	1.226	1.225	1.214
Q_1 (kJ/kg)	3399.6	3648.4	12,996.9	12,744.9	12,7728.0	12,622.4
V_D (m/s)	1997.95	2398.9	3334.7	3244.2	3241.5	3289.5

Table 4. Thermochemical properties during the reaction.

State 1 (Reactant)						
Properties	ACN	JET-A	MA	JSPK	CSPK	AL
c_{p1}	1.057	1.294	1.037	1.156	1.158	1.099
q_1	613.87	608.75	3412.21	2140.06	2147.67	2910.72
γ_1	1.379	1.267	1.209	1.226	1.225	1.214
State 2 (Product)						
c_{p2}	1.443	1.531	1.797	1.923	1.915	1.79
q_2	−2785.73	−3039.65	−9584.74	−10,604.9	−10,580.4	−9711.72
R_2	0.279	0.289	0.261	0.273	0.271	0.258
γ_2	1.24	1.232	1.17	1.165	1.165	1.168

4.3. Comparative Detonation Analysis of Alternative Biofuels Using ZND Model

The trend for the pressure ratio achieved by various alternative fuels at the minimum conditions of pressure, temperature, and mass flux is demonstrated in Figure 4a. It is clearly seen that two separate regions exist. One region is occupied by Microalgae Biofuel, CSPK, JSPK, and Algae Biofuel, while a lower region consists of Jet-A and acetylene. CSPK and JSPK Biofuels are hardly distinguishable and take almost identical values. All the fuels exhibit an initial increase in pressure ratio approaching the shock, and then this begins to diminish in the later phase. The strength of the pressure gained will weaken as the wave propagating back upstream and multiple cycles are taken into account. However these effects are not considered here. The graphs additionally show that biofuels are quite sensitive to detonation where there are vast changes in pressure ratio.

As presented in Figure 4b, the variation of the temperature ratio takes a different trend. All fuels exhibit a temperature increase along the detonation tube. The temperature ratio rises rapidly before the shock and then relaxes downstream. It is clear that a similar two regions exist in the temperature ratio variations field. After the shock takes place, CSPK and JSPK Biofuels achieve the highest change in temperature, followed by Microalgae Biofuel, Algae Biofuel, Jet-A, and Acetylene. Thus, in addition to the pressure-rise in detonation combustion, a temperature rise can also be accomplished.

The density ratio patterns demonstrate a similar trend to the pressure ratio, as shown in Figure 4c. All the biofuels (Microalgae Biofuel, Algae Biofuel, CSPK, and JSPK) exhibit a significant change in density compared to the other types of fuels, while acetylene shows the least variation in Stage 2. Compared to the previously discussed pressure and temperature ratio variations, the changes seen in the final stage are not very significant. The molecular structure of the fuel, enthalpy-formation of the reaction, and the initial conditions all affect these changes. The one-dimensional physical parameters obtained are consistent with the structure of a detonation wave as highlighted in Kuo [51].

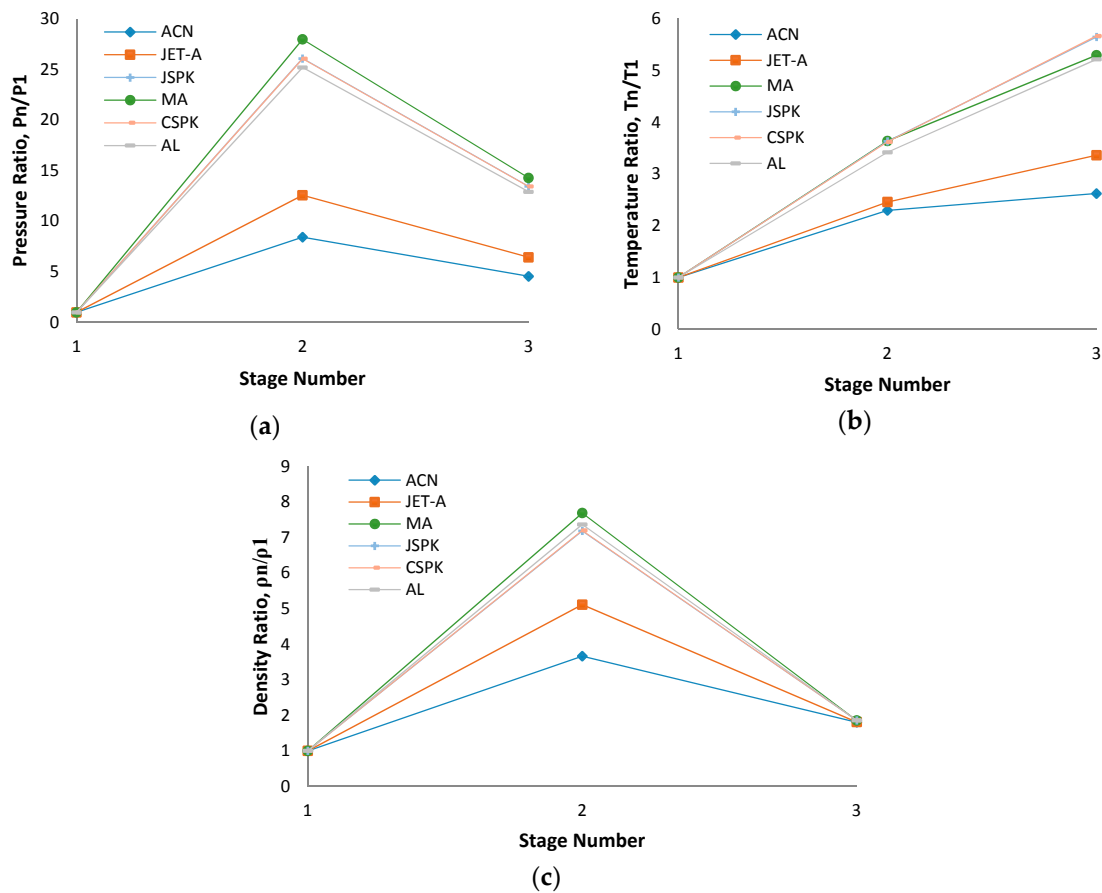


Figure 4. (a) Pressure ratios; (b) temperature ratios; and (c) density ratios at different stages.

4.4. Influence of Various Initial Conditions

Initial conditions are the crucial driving factors for the physical properties of burned gas at downstream locations. The impact of different upstream underlying conditions such as temperature, the mass flux and pressure on the pressure, temperature, specific volume, and Mach number ratios are discussed in this section to give a wider insight into how the initial conditions affect downstream physical properties. The ratios presented are for burned gas to unburned gas. Based on the quadratic functions considered above, there are two distinct physical phenomena, which occur in the form of weak and strong detonations. These are also derived from the upper Chapman-Jouget point. Turns [47] has characterized strong detonation as occurring when the burned gas velocity has a subsonic speed (above the upper CJ point), while weak detonation occurs when the burned gas velocity reaches supersonic speed (below the upper CJ point).

4.4.1. Effects of Initial Mass Flux

Further fuel comparisons have been made to investigate changes in physical properties as the mass flux increases. However, only strong shock influences are specifically presented and discussed here. Due to its high sensitivity, Acetylene fuel analysis is excluded from the discussion. The initial conditions for the pressure and temperature are specified as 1 atm and 2000 K, respectively. These parameters are chosen to correspond to when each of the fuels has accomplished its detonation velocity. Both the temperature and pressure ratios illustrate a linear increment for all fuels as the mass flux increases, as indicated by Figure 5a,b. JSPK and CSPK fuels appear to have the highest temperature ratio, while Jet-A fuel shows the highest pressure ratio. Due to their similar molecular formulae, JSPK and CSPK are again barely differentiated. The corresponding changes in specific volume and Mach

number ratios are illustrated in Figure 5c,d. All the alternative fuels have a specific volume reduction after the shock wave for the strong detonation condition. Relatively little variation of these two ratios is observed for Jet-A fuel. In contrast MA fuel shows significant changes in specific volume and Mach number ratios at low mass flux before these start to settle.

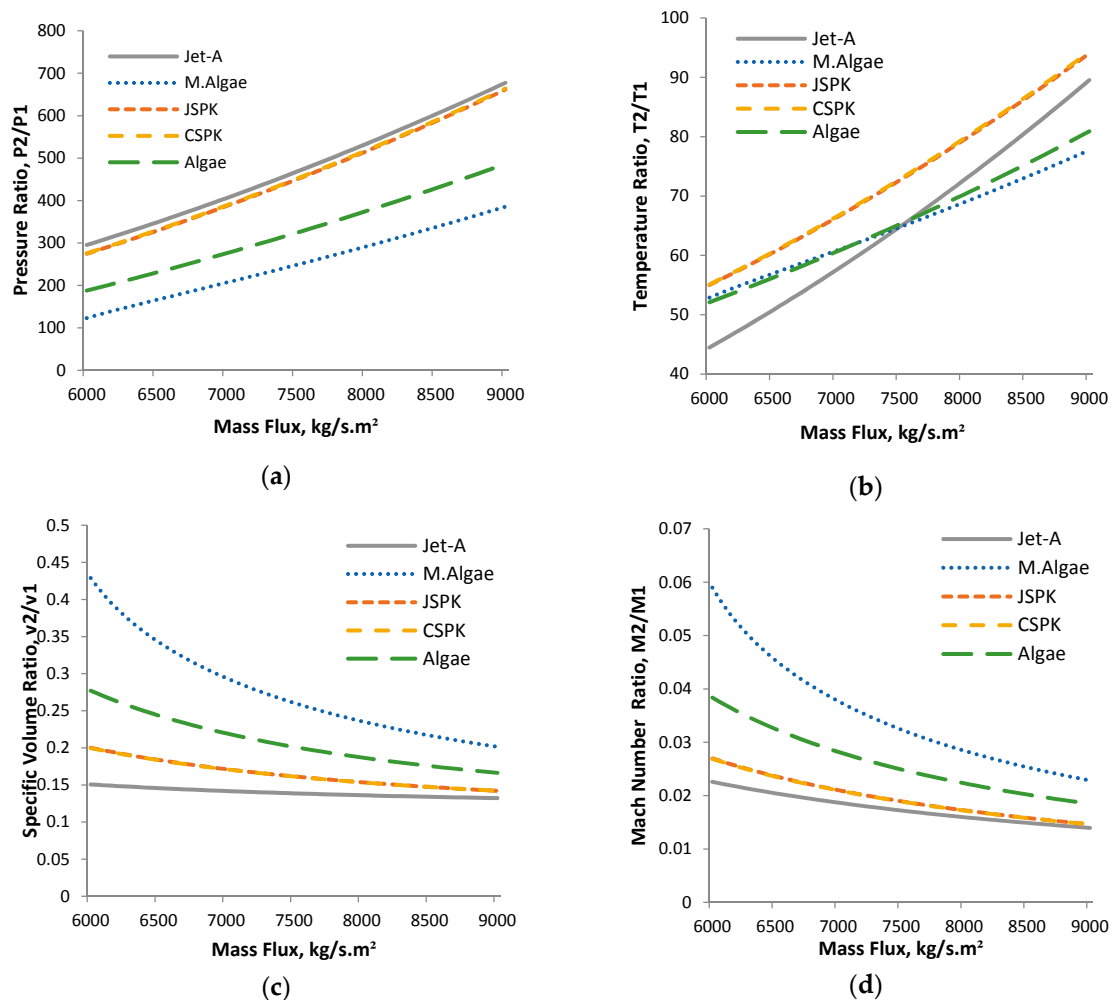


Figure 5. Comparison of (a) pressure ratios; (b) temperature ratios; (c) specific volume ratios; (d) and Mach number ratios at different initial mass flux under influence of strong detonation ($P = 1$ atm, $T = 2000$ K).

4.4.2. Effects of Initial Temperature

In this section, the impact of the initial temperature on the subsequent temperature, pressure, specific volume, and Mach number ratios are discussed. While the initial temperature varies, the other initial conditions for mass flux and pressure are held fixed. The initial temperature varies from 2000 K as this is the minimum temperature for MA and Algae Biofuel (AL) fuels to detonate. Figure 6a,b illustrate the resulting changes in pressure and temperature ratios, respectively. These demonstrate similar patterns to those seen with variations in mass flux but are less significant. This suggests that mass flux has a bigger impact on the pressure and temperature ratios, as reflected in the gradients seen on the corresponding graphs. Similarly, as the initial temperature increases, more significant temperature ratio variations were seen for detonation of Jet-A (Kerosene) compared to other fuels.

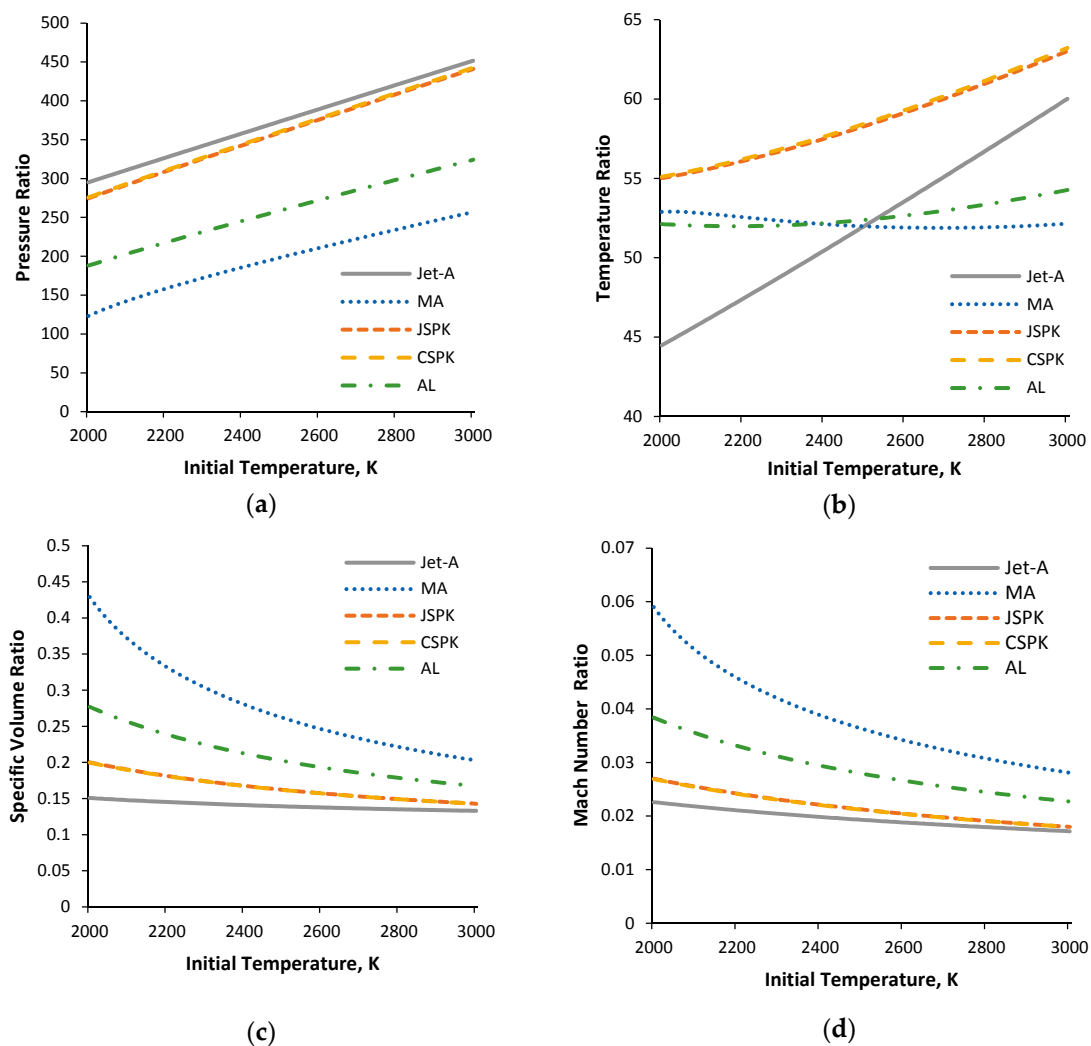


Figure 6. Comparison of (a) pressure ratios; (b) temperature ratios; (c) specific volume ratios; (d) and Mach number ratios at different initial temperature under influence of strong detonation ($P = 1 \text{ atm}$, $G = 6000 \text{ kg/s}\cdot\text{m}^2$).

The impact of the initial temperature on the specific volume and Mach number ratios is similar, but the gradients of changes with initial temperature are much higher (Figure 6c,d), and initial temperature has a more notable effect on the specific volume and Mach number ratios compared to the initial mass flux. It would require further modeling to explain the distinct changes to specific volume and Mach number ratios in Jet-A, JSPK, and CSPK fuels, but it appears that these fuels display more prominent gradient changes in the specific volume and Mach number ratios at the lowest temperature for detonation.

4.4.3. Effects of Initial Pressure

Initial pressure has a significant effect on the flow speed at the end of the tube significantly, as well as providing the limiting factor in its variation for detonation to occur. To portray the limitation, Microalgae fuel is chosen, and the initial temperature set to be 2000 K, while varying the mass fluxes between $6600 \text{ kg/s}\cdot\text{m}^2$ and $6200 \text{ kg/s}\cdot\text{m}^2$. Figure 7 plots the results based on the Mach number of the burned gas under both strong and weak shock conditions. At higher mass flux, the initial pressure can be raised across a wider range compared to that with lower mass flux. As the initial pressure rises, for a given mass flux, the burned gas Mach number increases in the case of a strong shock wave,

whereas a weak shock tends to reduce the burned gas flow. All the burned gas flows converge on the choking condition. Due to these restrictions, higher mass flux is preferred in comparison to other alternative fuels because these could impose severe limitations on the modelling.

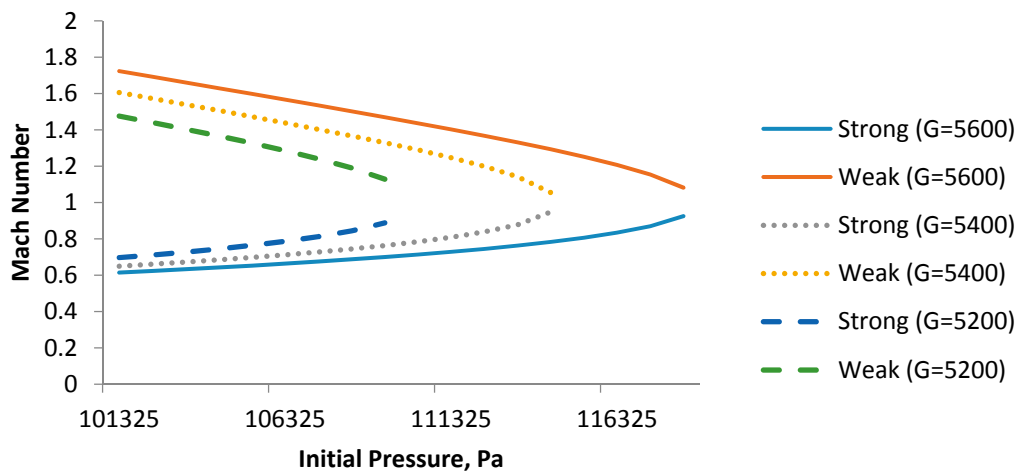


Figure 7. The influence of initial pressure and mass flux on the Mach number for Algae Biofuel (T = 2000 K).

In Figure 8, comparisons of other fuel options, based on temperature, pressure, Mach number, specific volume, and the ratios of Mach number, as affected by strong detonation waves, are presented. As mentioned previously, an exponential increase in burned gas Mach number and specific volume ratios results from interaction with such strong detonation. In particular, MA fuel is seen to be more sensitive to the changes of initial pressure than Jet-A fuel. A high starting pressure will result in a decrease in the pressure and temperature ratios. For a given mass flux, this could provide a limitation on the further reduction of the temperature and pressure ratio changes, particularly for MA fuel.

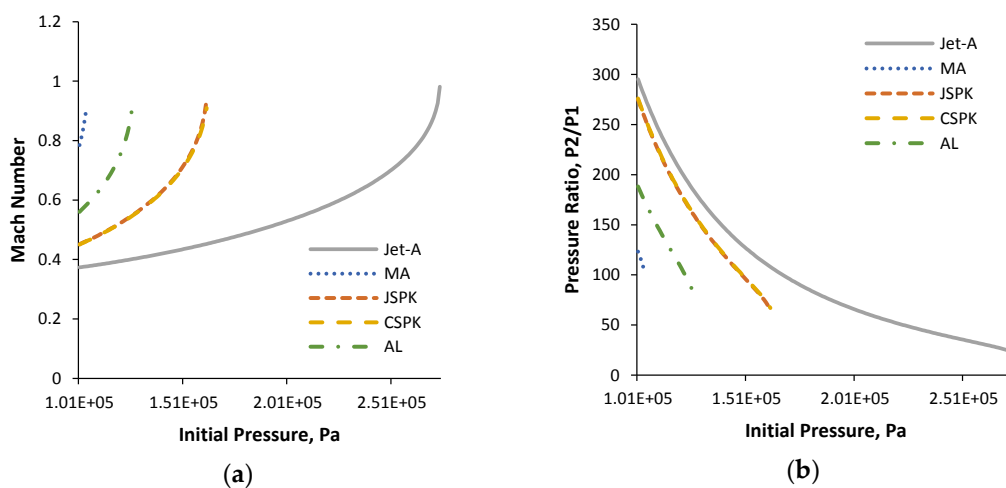


Figure 8. Cont.

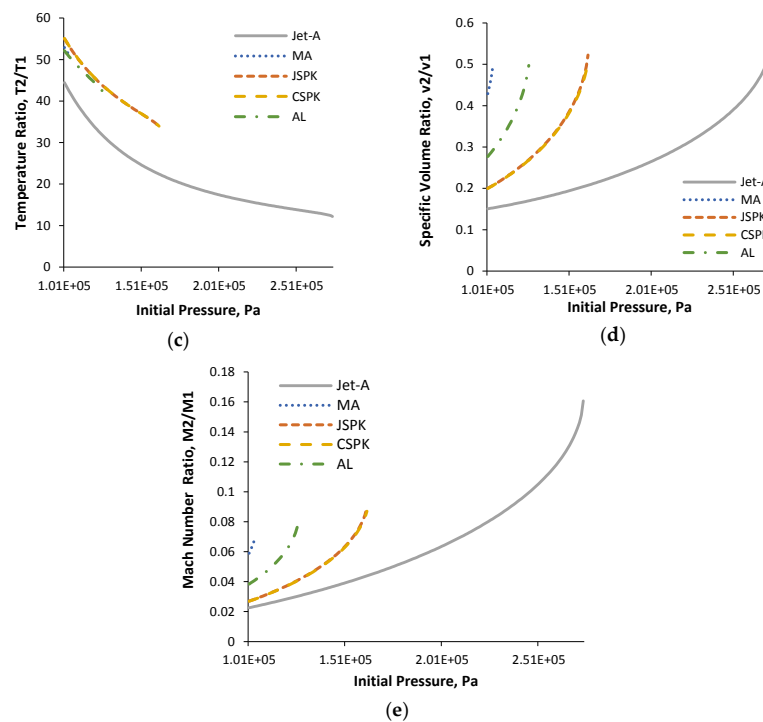


Figure 8. Comparison of (a) Mach number; (b) pressure ratios; (c) temperature ratios; (d) specific volume ratios; and (e) Mach number ratios at different initial pressure under influence of strong detonation ($T = 2000 \text{ K}$, $G = 6000 \text{ kg/s}\cdot\text{m}^2$).

5. Conclusions

The focus of this work was on the assessment of pulse detonation using alternative fuels. In awareness of the energy crisis and environmental concerns, and at the same time to promote performance and thermodynamic efficiency enhancement to the combustor, one-dimensional models of alternative fuels in a detonation mode of combustion are thoroughly discussed and presented. A comprehensive review has been made to highlight work that has been done in this area, and concerning the PDE process during operations. However, to the authors' knowledge, no research has been conducted to accommodate alternative fuels in PDE. Therefore, the present work has examined the feasibility and effectiveness of various alternative fuels under PDE conditions. By systematically treating the Rankine-Hugoniot Equation, Rayleigh Line Equation, and Zel'dovich–von Neumann–Doering model and taking into account single step chemistry and thermophysical properties for a stoichiometric mixture, the temporal effects of pressure, temperature, and density have been investigated, as well as the effect of different initial conditions. The main conclusions of the work are as follows:

1. Comparing each fuel at its detonation condition, the following trends in pressure, temperature, specific volume, and Mach number with initial mass flux, pressure, and temperature have been identified in Table 5 where \uparrow represents increase while \downarrow represents decrease in the physical properties.

Based on the model results obtained, it would appear that the pressure ratio shows the most significant changes, followed by the temperature ratio, specific volume ratio, and Mach number ratio.

2. The effects of mass flux variation imposed limitations on the changes in the initial pressure, with higher mass flux allowing a wider range of initial pressure variations. The initial temperature

had a significant effect on the specific volume and Mach number ratios, while the initial mass flux had a greater effect on both the pressure and temperature ratios.

- As expected, in terms of chemistry, heavier hydrocarbons in the form of the alternative bio-fuels considered here need much higher heat addition during the reaction to break the bonds of their more complex molecular structures and thus have greater molar specific heat. This was evidenced through a thermochemistry evaluation of the combustion flame temperature. When each fuel detonated, their behaviours exhibited different sensitivities. Since lighter fuels detonated more easily, further elevating initial conditions resulted in a much higher chemical reaction rate because more free atoms were then available for reaction.
- The chemical and physical analysis presented above can be extended to study the thrust chamber dynamic and propulsive performance of a pulse detonation engine running on alternative bio-fuels. To sustain detonation, careful geometrical sizing of the tube design will be required. The other important aspect that requires extensive attention in the future is the need also to evaluate and characterise pulse detonation engine emissions and thus pollutant formation.

Table 5. Effects of initial conditions to the burned states.

Properties	G↑		T↑		P↑	
	Strong	Weak	Strong	Weak	Strong	Weak
P_2	↑	↓	↑	↓	↓	↑
T_2	↑	↓	↑	↓	↓	↑
v_2	↓	↑	↓	↑	↑	↓
M_2	↓	↑	↓	↑	↑	↓

Acknowledgments: The first author, Muhammad Hanafi Azami acknowledges the sponsorship by International Islamic University Malaysia for funding his Ph.D. studies and also the Propulsion Engineering Centre, Cranfield University, UK for supporting the cost of the publication.

Author Contributions: All the authors have fully co-operated for the preparation of the work. Muhammad Hanafi Azami designed the numerical framework for the alternative fuels. Both authors, Muhammad Hanafi Azami and Mark Savill analyze, validate and carried out uncertainties analysis of the results.

Conflicts of Interest: The authors declare no conflict of interest.

Nomenclature

AL	algae biofuel
$CSPK$	Camelina Bio-synthetic Paraffinic Kerosene
C_2H_2	Acetylene
c_p	Constant Pressure Specific Heat (J/kg·K)
\bar{c}_p	Tabulated Constant Pressure Specific Heat (J/kg·K)
h_f^0	Enthalpy of Formation (J/kg)
G	Mass flux (kg/s·m ²)
$JSPK$	Jatropha Bio-synthetic Paraffinic Kerosene
M	Mach number
MA	Microalgae Biofuel
MW	Molecular Weight (kg/mol)
\dot{m}''	Mass Flow Rate Second Order (kg/s)
P	Pressure (Pa)
PDE	Pulse Detonation Engine

q	Heat Addition (J/kg)
R	Specific Gas Constant (J/kg·K)
R_u	Universal Gas Constant (J/kmol·K)
T	Temperature (K)
V	Velocity (m/s)
V_D	Detonation Velocity (m/s)
v	Specific Volume (m ³ /kg)
Y	Mass Fraction
γ	Specific Heat Ratio
ρ	Density (kg/m ³)
χ	Mole Fraction
Subscript	
1	State 1
2	State 2
2'	State 2' (arbitrary)
i	Species number
x	Axial direction

Appendix

Table A1. Thermochemical properties for alternative fuels used.

	MICROALGAE	ALGAE	JATROPHA	CAMELINA
Density (kg/m ³)	886	883.6	864–880	-
Cetane Number	48.31	85–92	46–55	50.4
Viscosity (mm ² /s @ 40)	4.47	4.73	3.7–5.8	3.80
Pour Point (°)	−12	−21–−24	5	−7
Flash Point (°)	165.5	179	163–238	136
Heating Value (MJ/kg)	40.045	40.72	38.5–42	45.2
CFPP (°)	18	-	−1.2	−3
Acid Value (mg/KOH)	0.13	0.37	0.34	-
Cloud point (°)	−5.2	7	5	3
C (%)	61.52	68.30	76.57	-
H (%)	8.50	8.30	12.21	-
O (%)	20.19	16.40	11.32	-
N (%)	9.79	6.20	-	-
Kinematic viscosity (mm ² /s ² @ 40)	33.06	-	4.75	-
Oxidation stability (h)	8.83	6.76	5.0	-
Iodine Value (g I ₂ /100 g)	119.1 g	97.12	109.5	152.8
Sulfur Content (ppm)	-	8.1	12.9	-
Specific Gravity	-	1.02 g/mL	0.876	0.882
References	[28,29,52–56]	[57–60]	[61–63]	[63]

References

1. Kentfield, J.A.C. Fundamentals of Idealized Airbreathing Pulse-Detonation Engines. *J. Propuls. Power* **2002**, *18*, 77–83. [[CrossRef](#)]

2. Eidelman, S.; Grossmann, W.; Lottati, I. Review of propulsion applications and numerical simulations of the pulsed detonation engine concept. *J. Propuls. Power* **1991**, *7*, 857–865. [[CrossRef](#)]
3. Ma, F.; Choi, J.; Yang, V. Thrust Chamber Dynamics and Propulsive Performance of Single-Tube Pulse Detonation Engines. In Proceedings of the 42nd AIAA Aerospace Sciences Meeting and Exhibit, Reno, NV, USA, 5–8 January 2004.
4. Kaemming, T. Integrated Vehicle Comparison of Turbo-Ramjet Engine and Pulsed Detonation Engine. *J. Eng. Gas Turbines Power* **2003**, *125*, 257–262. [[CrossRef](#)]
5. Qiu, H.; Xiong, C.; Yan, C.; Fan, W. Propulsive Performance of Ideal Detonation Turbine Based Combined Cycle Engine. *J. Eng. Gas Turbines Power* **2012**, *134*, 81201. [[CrossRef](#)]
6. Ebrahimi, H.B.; Merkle, C.L. Numerical Simulation of a Pulse Detonation Engine with Hydrogen Fuels. *J. Propuls. Power* **2002**, *18*, 1042–1048. [[CrossRef](#)]
7. Li, J.; Fan, W.; Yan, C.; Li, Q. Experimental Investigations on Detonation Initiation in a Kerosene-Oxygen Pulse Detonation Rocket Engine. *Combust. Sci. Technol.* **2009**, *181*, 417–432. [[CrossRef](#)]
8. Li, C.; Kailasanath, K. A Numerical Study of Reactive Flows in Pulse Detonation Engines. In Proceedings of the 37th AIAA/ASME/SAE/ASEE Joint Propulsion Conference & Exhibit, Salt Lake City, UT, USA, 8–11 July 2011.
9. Frolov, S.M. Natural-Gas-Fueled Pulse-Detonation Combustor. *J. Propuls. Power* **2014**, *30*, 41–46. [[CrossRef](#)]
10. Li, J.-M.; Teo, C.J.; Lim, K.S.; Wen, C.-S.; Khoo, B.C. Deflagration to Detonation Transition by Hybrid Obstacles in Pulse Detonation Engines. In Proceedings of the 49th AIAA/ASME/SAE/ASEE Joint Propulsion Conference AIAA, San Jose, CA, USA, 14–17 July 2013.
11. Wu, Y.; Ma, F.; Yang, V. System Performance and Thermodynamic Cycle Analysis of Air-Breathing Pulse Detonation Engines. In Proceedings of the 40th AIAA Aerospace Sciences Meeting & Exhibit, Reno, NV, USA, 14–17 January 2002.
12. Hutchins, T.E.; Metghalchi, M. Energy and Exergy Analyses of the Pulse Detonation Engine. *J. Eng. Gas Turbines Power* **2003**, *125*, 1075. [[CrossRef](#)]
13. Nikitin, V.F.; Dushin, V.R.; Phylippov, Y.G.; Legros, J.C. Pulse detonation engines: Technical approaches. *Acta Astronaut.* **2009**, *64*, 281–287. [[CrossRef](#)]
14. Panicker, P.K.; Wilson, D.R.; Lu, F.K. Operational Issues Affecting the Practical Implementation of Pulsed Detonation Engines. In Proceedings of the 14th AIAA/AHI Space Planes and Hypersonic Systems and Technologies Conference, Canberra, Australia, 6–9 November 2006.
15. New, T.; Panicker, P.; Chui, K.; Tsai, H.; Lu, F. Experimental Study on Deflagration-to-Detonation Transition Enhancement Methods in a PDE. In Proceedings of the 14th AIAA/AHI Space Planes and Hypersonic Systems and Technologies Conference, Canberra, Australia, 6–9 November 2006.
16. Kailasanath, K.; Patnaik, G.; Li, C. The flowfield and performance of pulse detonation engines. *Proc. Combust. Inst.* **2002**, *29*, 2855–2862. [[CrossRef](#)]
17. Tucker, K.C.; King, P.I.; Schauer, F.R. Hydrocarbon Fuel Flash Vaporization for Pulsed Detonation Combustion. *J. Propuls. Power* **2008**, *24*, 788–796. [[CrossRef](#)]
18. Harris, P.G.; Guzik, S.; Farinaccio, R.; Stowe, R.A.; Whitehouse, D.; Josey, T.; Hawkin, D.; Ripley, R.; Link, R.; Higgins, A.; et al. Comparative Evaluation of Performance Models of Pulse Detonation Engines. In Proceedings of the 38th AIAA/ASME/SAE/ASEE Joint Propulsion Conference & Exhibit, Indianapolis, Indiana, USA, 7–10 July 2002.
19. Caldwell, N.; Gutmark, E. A Review of Pulse Detonation Engine Research at the University of Cincinnati. In Proceedings of the 43rd AIAA/ASME/SAE/ASEE Joint Propulsion Conference & Exhibit, Cincinnati, OH, USA, 8–11 July 2007.
20. Vutthivithayarak, R.; Braun, E.M.; Lu, F.K. Examination of the Various Cycles for Pulse Detonation Engines. In Proceedings of the 47th AIAA/ASME/SAE/ASEE Joint Propulsion Conference & Exhibit, San Diego, CA, USA, 31 July–3 August 2011.
21. Singleton, D.R.; Sinibaldi, J.O.; Brophy, C.M.; Kuthi, A.; Gundersen, M.A. Compact Pulsed-Power System for Transient Plasma Ignition. *IEEE Trans. Plasma Sci.* **2009**, *37*, 2275–2279. [[CrossRef](#)]
22. Lu, F.K.; Carter, J.D.; Wilson, D.R. Development of a Large Pulse Detonation Engine Demonstrator. In Proceedings of the 47th AIAA/ASME/SAE/ASEE Joint Propulsion Conference & Exhibit, San Diego, CA, USA, 31 July–3 August 2011.

23. Hinkey, J.; Williams, J.; Henderson, S.; Bussing, T. Rotary-valved, multiple-cycle, pulse detonation engine experimental demonstration. In Proceedings of the 33rd Joint Propulsion Conference and Exhibit, Seattle, WA, USA, 6–9 July 1997.
24. Panicker, P.K.; Li, J.-M.; Lu, F.K.; Wilson, D.R. Development of a Compact Liquid Fueled Pulsed Detonation Engine with Predetonator. In Proceedings of the 45th AIAA Aerospace Sciences Meeting and Exhibit, Reno, NV, USA, 8–11 January 2007.
25. Brophy, C.M. Initiation Improvements for Hydrocarbon/Air Mixtures in Pulse Detonation Applications. In Proceedings of the 47th AIAA Aerospace Sciences Meeting Including The New Horizons Forum and Aerospace Exposition, Orlando, FL, USA, 5–8 January 2009.
26. Li, C.; Kailasanath, K. Detonation Initiation in Pulse Detonation Engines. In Proceedings of the 41st Aerospace Sciences Meeting and Exhibit, Reno, NV, USA, 6–9 January 2003.
27. Lü, J.; Sheahan, C.; Fu, P. Metabolic engineering of algae for fourth generation biofuels production. *Energy Environ. Sci.* **2011**, *4*, 2451. [[CrossRef](#)]
28. Brennan, L.; Owende, P. Biofuels from microalgae—A review of technologies for production, processing, and extractions of biofuels and co-products. *Renew. Sustain. Energy Rev.* **2010**, *14*, 557–577. [[CrossRef](#)]
29. Atabani, A.E.; Silitonga, A.S.; Badruddin, I.A.; Mahlia, T.M.I.; Masjuki, H.H.; Mekhilef, S. A comprehensive review on biodiesel as an alternative energy resource and its characteristics. *Renew. Sustain. Energy Rev.* **2012**, *16*, 2070–2093. [[CrossRef](#)]
30. Huang, G.; Chen, F.; Wei, D.; Zhang, X.; Chen, G. Biodiesel production by microalgal biotechnology. *Appl. Energy* **2010**, *87*, 38–46. [[CrossRef](#)]
31. Mata, T.M.; Martins, A.A.; Caetano, N.S. Microalgae for biodiesel production and other applications: A review. *Renew. Sustain. Energy Rev.* **2010**, *14*, 217–232. [[CrossRef](#)]
32. Suali, E.; Sarbatly, R. Conversion of microalgae to biofuel. *Renew. Sustain. Energy Rev.* **2012**, *16*, 4316–4342. [[CrossRef](#)]
33. Rawat, I.; Kumar, R.R.; Mutanda, T.; Bux, F. Biodiesel from microalgae: A critical evaluation from laboratory to large scale production. *Appl. Energy* **2013**, *103*, 444–467. [[CrossRef](#)]
34. Heiser, W.H.; Pratt, D.T. Thermodynamic Cycle Analysis of Pulse Detonation Engines. *J. Propuls. Power* **2002**, *18*. [[CrossRef](#)]
35. Kentfield, J.A.C. Thermodynamics of Airbreathing Pulse-Detonation Engines. *J. Propuls. Power* **2002**, *18*, 1170–1175. [[CrossRef](#)]
36. Brophy, C.M.; Sinibaldi, J.O.; Damphousse, P. Initiator Performance for Liquid-Fueled Pulse Detonation Engines. In Proceedings of the 40th AIAA Aerospace Sciences Meeting & Exhibit, Reno, NV, USA, 14–17 January 2002.
37. Wintenberger, E.; Shepherd, J.E. A Model for the Performance of Air-Breathing Pulse Detonation Engines. In Proceedings of the 39th AIAA/ASME/SAE/ASEE Joint Propulsion Conference and Exhibit, Huntsville, AL, USA, 20–23 July 2003; Volume 1, pp. 1–16.
38. Blanco, G.M. *Numerical Modelling of Pressure Rise Combustion for Reducing Emissions of Future Civil Aircraft*; Cranfield University: Cranfield, UK, 2014.
39. Kailasanath, K. Review of Propulsion Application of Detonation Waves. *AIAA J.* **2000**, *38*, 1698–1708. [[CrossRef](#)]
40. Li, J.; Fan, W.; Qiu, H.; Yan, C.; Wang, Y.-Q. Preliminary study of a pulse normal detonation wave engine. *Aerosp. Sci. Technol.* **2010**, *14*, 161–167. [[CrossRef](#)]
41. Ma, F.; Choi, J.-Y.; Yang, V. Propulsive Performance of Airbreathing Pulse Detonation Engines. *J. Propuls. Power* **2006**, *22*, 1188–1203. [[CrossRef](#)]
42. Roy, G.D.; Frolov, S.M.; Borisov, A.A.; Netzer, D.W. Pulse detonation propulsion: Challenges, current status, and future perspective. *Prog. Energy Combust. Sci.* **2004**, *30*, 545–672. [[CrossRef](#)]
43. Kailasanath, K. Recent Developments in the Research on Pulse Detonation Engines. *AIAA J.* **2003**, *41*, 145–159. [[CrossRef](#)]
44. Kailasanath, K. Liquid-Fueled Detonations in Tubes. *J. Propuls. Power* **2006**, *22*, 1261–1268. [[CrossRef](#)]
45. Shimada, T.; Hayashi, A.K.; Yamada, E.; Tsuboi, N. Numerical Study on Detonation Characteristics Using a Bio-Fuel. In Proceedings of the 49th AIAA Aerospace Sciences Meeting including the New Horizons Forum and Aerospace Exposition, Orlando, FL, USA, 4–7 January 2011.

46. Dairobi, G.; Wahid, M.A.; Inuwa, I.M. Feasibility Study of Pulse Detonation Engine Fueled by Biogas. *Adv. Thermofluids* **2013**, *388*, 257–261. [[CrossRef](#)]
47. Turns, S. *Introduction to Combustion: Concepts and Application*; McGraw-Hill: Singapore, 2000.
48. Wintenberger, E.; Austin, J.M.; Cooper, M.; Jackson, S.; Shepherd, J.E. Analytical Model for the Impulse of Single-Cycle Pulse Detonation Tube. *J. Propuls. Power* **2003**, *19*, 22–38. [[CrossRef](#)]
49. Yungster, S.; Breisacher, K. Study of NO_x Formation in Hydrocarbon-Fuelled Pulse Detonation Engines. In Proceedings of the 41st AIAA/ASME/SAE/ASEE Joint Propulsion & Exhibit, Tucson, AZ, USA, 10–13 July 2005.
50. Cheatham, S.; Kailasanath, K. Single-Cycle Performance of Idealized Liquid-Fueled Pulse Detonation Engines. *AIAA J.* **2005**, *43*, 1276–1283. [[CrossRef](#)]
51. Kuo, K. *Principles of Combustion*, 2nd ed.; John Wiley & Sons: Hoboken, NJ, USA, 2005.
52. Tüccar, G.; Aydın, K. Evaluation of methyl ester of microalgae oil as fuel in a diesel engine. *Fuel* **2013**, *112*, 203–207. [[CrossRef](#)]
53. Amin, S. Review on biofuel oil and gas production processes from microalgae. *Energy Convers. Manag.* **2009**, *50*, 1834–1840. [[CrossRef](#)]
54. Chen, Y.-H.; Huang, B.-Y.; Chiang, T.-H.; Tang, T.-C. Fuel properties of microalgae (*Chlorella protothecoides*) oil biodiesel and its blends with petroleum diesel. *Fuel* **2012**, *94*, 270–273. [[CrossRef](#)]
55. Rinaldini, C.A.; Mattarelli, E.; Magri, M.; Beraldi, M. *Experimental Investigation on Biodiesel from Microalgae as Fuel for Diesel Engines*; SAE Technical Paper; SAE International: USA, 2014.
56. Ahmad, A.L.; Mat Yasin, N.H.; Derek, C.J.C.; Lim, J.K. Microalgae as a sustainable energy source for biodiesel production: A review. *Renew. Sustain. Energy Rev.* **2011**, *15*, 584–593. [[CrossRef](#)]
57. Makarevičienė, V.; Lebedevas, S.; Rapalis, P.; Gumbyste, M.; Skorupskaite, V.; Žaglinskis, J. Performance and emission characteristics of diesel fuel containing microalgae oil methyl esters. *Fuel* **2014**, *120*, 233–239. [[CrossRef](#)]
58. Alcaine, A.A. Biodiesel from microalgae. *Biotechnol. Adv.* **2007**, *25*, 294–306.
59. Haik, Y.; Selim, M.Y.E.; Abdulrehman, T. Combustion of algae oil methyl ester in an indirect injection diesel engine. *Energy* **2011**, *36*, 1827–1835. [[CrossRef](#)]
60. Jena, U.; Vaidyanathan, N.; Chinnasamy, S.; Das, K.C. Evaluation of microalgae cultivation using recovered aqueous co-product from thermochemical liquefaction of algal biomass. *Bioresour. Technol.* **2011**, *102*, 3380–3387. [[CrossRef](#)] [[PubMed](#)]
61. Ashraful, A.M.; Masjuki, H.H.; Kalam, M.A.; Fattah, I.M.R.; Imtenan, S.; Shahir, S.A.; Mobarak, H.M. Production and comparison of fuel properties, engine performance, and emission characteristics of biodiesel from various non-edible vegetable oils: A review. *Energy Convers. Manag.* **2014**, *80*, 202–228. [[CrossRef](#)]
62. Giakoumis, E.G. A statistical investigation of biodiesel physical and chemical properties, and their correlation with the degree of unsaturation. *Renew. Energy* **2013**, *50*, 858–878. [[CrossRef](#)]
63. Hoekman, S.K.; Broch, A.; Robbins, C.; Cenicerros, E.; Natarajan, M. Review of biodiesel composition, properties, and specifications. *Renew. Sustain. Energy Rev.* **2012**, *16*, 143–169. [[CrossRef](#)]



Pulse detonation assessment for alternative fuels

Azami, Muhammad Hanafi

2017-03-15

Attribution 4.0 International

Azami MH, Savill M. (2017) Pulse detonation assessment for alternative fuels. *Energies*, Volume 10, Issue 3, March 2017, Article number 369

<http://dx.doi.org/10.3390/en10030369>

Downloaded from CERES Research Repository, Cranfield University